Hollow Carbon Nanospheres with Superior Rate Capability for Sodium-Based Batteries

Kun Tang, Lijun Fu, Robin J. White, Linghui Yu, Maria-Magdalena Titirici, Markus Antonietti, and Joachim Maier**

New energy technologies are critical to address global concerns regarding energy shortages and environmental issues. Lithium-based batteries are currently the technology of choice to develop renewable energy technology and electric vehicles due to their high energy density. In this context, if electric vehicles are to gain a significant share of future automobile markets, battery production and, therefore, the demand of lithium must grow proportionately and perhaps unsustainably. Therefore there is growing concern regarding the increasing cost and an uneven geological distribution of lithium source in recent years.[1]

Contrary to the tremendous study, research and commercial success of the lithium-ion battery, there has been a relative dearth of studies on other alkaline earth metal systems such as the sodium-ion battery.[2–5] The system is one possible alternative to the lithium-ion battery due to the low cost and comparatively higher natural abundance of sodium, particularly with regard to large-scale applications. Recently, sodium-ion batteries were revisited by several groups, which were mainly focused on cathode materials, including $NaCrO_2$, $NaTi_2(PO_4)_3$ and $Na(Ni_{0.5}Mn_{0.5})O_2$.[6–8] It has been well established that only a small amount of sodium can intercalate to graphite, which is the dominant anode material in today's commercial lithium rechargeable batteries.[9,10] Generally, increasing the graphitization degree results in decay of the sodium storage capacity.[11,12] As a result, disordered carbon appears to be the most suitable anode material for sodium ion batteries.

Classically, lithium batteries employ various different types of materials as anodes including carbonaceous materials, lithium alloys and metal oxides et al., whilst disordered carbon is now considered the dominant candidate material for sodium ion batteries for a number of reasons. Very recently, Chevrier and Ceder evaluated the possibility of exploring sodium alloys as negative electrode for sodium ion batteries, but no experimental data has thus far been forthcoming.[13] The electrochemical insertion of sodium ions into carbon (e.g. petroleum-coke) as first studied by Doeff et al.,[14] was reported to generate a reversible capacity of ~85 $mAhg^{-1}$. Subsequent works on various type of carbonaceous materials have demonstrated that sodium ion uptake in disordered carbon showed similar charge/discharge curves as with lithium, but present in general a lower capacity due to the larger comparative ion diameter of sodium.[11,12,15–18] The highest reversible sodium capacity of 300 $mAhg^{-1}$ (with sodium plating) was achieved for hard carbons derived from ball-milled sugars, as reported by Stevens and Dahn.[16] However, the cyclability and rate capability of these materials in previous studies are insufficient, whilst the majority of these studies were also performed under either very low current density or high temperatures, which are still far from the ideal operation conditions to make a serious market and application impact for sodium ion batteries.

As Dahn et al. suggested, the sodium storage mechanism in disordered carbon can be considered similar to that of lithium and therefore it is logical to take note of the success of strategies applied to disordered carbon for lithium battery anodes.[10] In this context, Maier has addressed the critical impact of interface and size effects on mass transfer, transport and storage, tuning particle size and morphology on the optimization of electrochemical performance.[19] More recently Wenzel et al. have demonstrated the use of hierarchically porous carbon monoliths as high rate anode materials for sodium ion batteries, which were once used as high rate anode materials for lithium ion batteries before.[20,21] However, the relatively low capacity (i.e. 130 $mAhg^{-1}$ at 0.0744 Ag^{-1}) remains to be improved.

Recently hollow nanospheres have been demonstrated to be an attractive carbon material morphology in lithium ion batteries, since the unique hollow structure may boost mass transport by offering a large surface area and a short diffusion distance.[22–25] Herein, we report for the first time the use of hollow carbon nanospheres as sodium ion battery anode materials. The hollow carbon nanospheres were synthesized using a facile, sustainable method based on hydrothermal carbonization of glucose in the presence of latex templates. The hydrothermal decomposition of Glucose yields a thin layer of hydrothermal carbon around the latex template, whilst further non-oxidative thermal treatment at 1000 °C, removes the template core to produce hollow carbon spheres with thin amorphous carbon walls. The resulting void volume roughly conforms (taking into account carbon shell contraction) with the original latex template size, whilst the thickness of the carbon shell is ca. 12 nm.[26] In this paper we have investigated for the first time the electrochemical performance of hollow carbon nanospheres as sodium ion battery anode material.

Dr. K. Tang, Dr. L. Fu, Prof. J. Maier
Max Planck Institute for Solid State Research
Heisenbergstr. 1.70569, Stuttgart, Germany
E-mail: s.weiglein@fkf.mpg.de
Dr. R. J. White, L. Yu, Dr. M.-M. Titirici,
Prof. M. Antonietti
Max Planck Institute for Colloids and Interfaces
Am Muehlenberg, 14476, Golm, Germany
E-mail: robin.white@mpikg.mpg.de
Dr. L. Fu
Shanghai Institute of Ceramics
Chinese Academy of Sciences
1295 Ding Xi Road, 200050, Shanghai, China

DOI: 10.1002/aenm.201100691

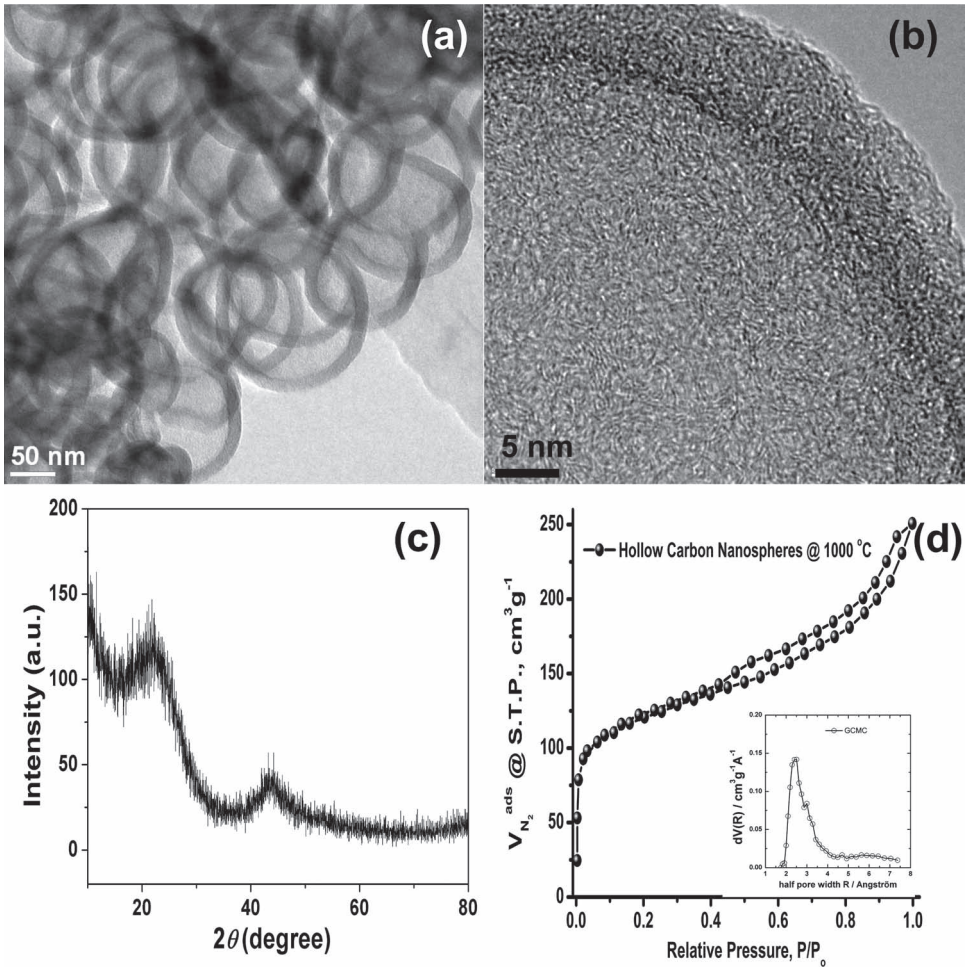

Figure 1. (a) TEM image and (b) HR-TEM image of hollow carbon nanospheres, (c) XRD pattern of hollow carbon nanospheres, (d) N_2 sorption isotherm and pore-size distribution curve (inset) from CO_2 sorption of the hollow carbon nanospheres.

Morphologically, electron micrograph image analysis indicates, as previously reported, uniformly shaped hollow nanospheres, which are neatly interlinked with each other, typically at the sphere surface (**Figure 1**a). Examination of the carbon shell by high-resolution transmission electron microscopy (HR-TEM) and X-ray diffraction (XRD) indicated a weakly ordered turbostratic carbon structuring (Figure 1b,c). The disordered graphitic-like shell thickness is ~12 nm, composed of ~2–3 short carbon layers. The XRD pattern presented two weak, broad diffraction peaks corresponding to the (002) and (100) diffraction modes at about 22.2° and 43.9°, characteristic of a disordered carbonaceous structure. This is typical for hydrothermal carbons in general due to their different formation mechanism and final chemical structure.[27] The interlayer spacing (d_{002}) was calculated as ~0.401 nm, which importantly in the context of ion insertion, is significantly wider than that classically observed for the model carbon, graphite (i.e. 0.336 nm). It is worthwhile to emphasize the importance of the difference in interlayer spacing. The occurrence of large free space between graphene layers should in principle be beneficial for the reversible storage of sodium considering the larger diameter of sodium ion (0.95 Å) compared to that of lithium ion (0.60 Å).

N_2 sorption analysis characterized the specific surface of the hollow carbon nanospheres investigated here as 410 m^2g^{-1}, whilst the sorption profile presented a reversible hysteresis loop (Figure 1d). CO_2 sorption analysis provided a more detailed analysis of the nanosphere shell microporosity (Figure 1d inset). The corresponding pores size distribution (PSD) analyzed using a GCMC/NLDFT model presented a relatively narrow micropore feature centered around a micropore entrance size of 0.2–0.35 nm.[28]

It is thought that the presented hollow nanospheres structure endows the material with excellent sodium storage performance. Cyclic voltammetry (CV) and galvanostatic discharge/charge cycling were performed to characterize the sodium ion insertion/extraction properties (**Figure 2**). In the first CV cycle, pronounced cathodic peaks were observed at 1.39 V, 0.36 V and near 0 V (Figure 2a). The peak at 1.39 V is attributed to the reaction of sodium with functional group(s) at the carbon surface, behaviour reported previously for lithium storage mechanisms for carbonaceous materials.[29] It is important to note a cathodic peak shift to lower voltage (i.e. 1.36 V) and a reduction of overall intensity over subsequent cycles indicating a partly reversible characteristic of this reaction. It is well known that propylene

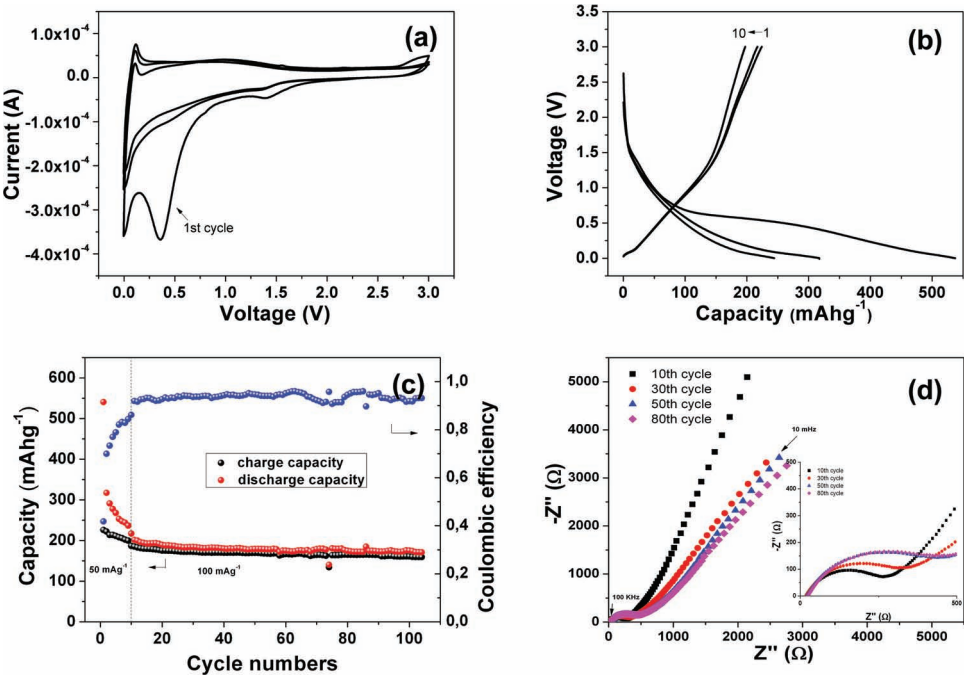

Figure 2. (a) CV of hollow carbon nanospheres showing the first three cycles between 3 V and 0 V at a scan rate of 0.1 mVs^{-1}, (b) Galvanostatic charge/discharge curves at a current rate of 50 mAg^{-1}, (c) Cycle performance of hollow carbon nanospheres, (d) Impedance spectra of hollow carbon nanospheres electrode after 10^{th}, 30^{th}, 50^{th}, and 80^{th} cycle. The inset is the enlarged spectra.

carbonate (PC) decomposes at ca. 0.7 V in lithium battery systems depending on electrode materials.[30,31] Considering the standard electrode potential difference, E^0 (Li/Li^+) - E^0(Na/Na^+), is 0.33 V for aqueous solutions and reported to be slightly smaller for PC (0.23 V) and similar value for ethylene carbonate (EC),[32] it is plausible to assign the cathodic peak at 0.36 V to PC decomposition, leading to the formation of a solid electrolyte interphase (SEI) as compared to the lithium system.[25] The clear sodium insertion peak observed at lower voltages near 0 V is similar for lithium insertion in carbonaceous materials.[33] Furthermore, a clear peak at 0.11 V in the reverse cycle is observed, a feature attributed to sodium extraction from shell nanopores (discussed later). However, sodium removal occurs over a broad potential range, similarly to previously reported lithium systems.[25]

The first discharge/charge cycle delivered specific capacities of 537 and 223 $mAhg^{-1}$ respectively at a current rate of 50 mAg^{-1} (Figure 2b). The large irreversible capacity arises from both electrolyte decomposition at the electrode/electrolyte surface and the irreversible insertion of sodium into potentially unique shell positions as demonstrated by features in the corresponding CV curves, which is interestingly analogous to previous literature discussions regarding lithium storage in disordered carbons.[34] The reversible capacity of 200 $mAhg^{-1}$ at a current density of 50 mAg^{-1} is significant, and only a few reports achieved capacities more than 200 $mAhg^{-1}$ for sodium anode materials, typically obtained at much lower current densities than that reported here.[11,16,18] And a reversible capacity of 150 $mAhg^{-1}$ can be obtained at voltage range 0–1.5 V, which is more suitable for practical application. The sloping charge curves in following cycles is somewhat similar to lithium insertion/ extraction except for the obvious plateau below 0.1 V observed here found for sodium extraction, which corresponds well with the anodic peak at 0.11 V in the reported CV curves. Previously reported studies have suggested two predominant mechanisms for sodium insertion into carbon; (1) Insertion of sodium between graphene layers corresponding to the sloping voltage profile and (2) Insertion into micropores at the lowest potentials.[10,12,16] It should be mentioned that, in our case, the sodium insertion into nanopores contributes less than 20 $mAhg^{-1}$ to the total sodium storage, with the majority of the capacity arising due to sodium insertion between graphene layers. Considering the favourable insertion of the sodium ion into the graphene layers with large interlayer spacing, it can be expected that a large fraction of sodium storage between graphene layers has a beneficial effect on the rate performance.

The cycling stability during sodium insertion/extraction in the hollow carbon nanospheres was also investigated at a current density of 50 mAg^{-1} for the first ten cycles and then 100 mAg^{-1} for subsequent cycles (Figure 2c). It is thought that the observed capacity loss over the initial cycling steps stems from SEI film stabilization and irreversible sodium ion insertion. After 100 cycles, a reversible capacity of ~160 $mAhg^{-1}$ is stably maintained. The coulombic efficiency approaches ~ 94% after several cycles, whilst the observed irreversible capacity during each cycle is attributed to the incomplete stabilization of SEI for the presented sodium battery system. The electrochemical impedance spectra of the hollow carbon nanospheres electrode was measured (Figure 2d). The Nyquist plots consist of a depressed semicircle in the high- and middle-frequency regions and a straight line in the low-frequency region. The semicircle can be attributed to the SEI film and contact resistance at high frequencies and a charge-transfer process in the middle-frequency, while the

linear increase in the low-frequency range may reflect Warburg impedance associated with sodium ion diffusion in the carbon electrode.[35] The charge-transfer resistances (R_{ct}) simulated from the equivalent circuits are 282, 337, 460 and 464 Ω after 10th, 30th, 50th, and 80th cycles, respectively (Supporting Information (SI), Figure S1). The carbon electrode shows an increase in resistance in the first 50 cycles and then achieves a steady state. This phenomenon is interpreted as the result o subsequent stable SEI formation throughout cycling. In this context it is important to note that this behaviour could potentially be improved via optimization of the electrolyte employed. Such a good cycling performance of >100 cycles has seldom been achieved in previous reports on anode materials for sodium ion batteries.[8]

Remarkably the reversible capacities at various discharge/charge rates, are retained at 168, 142, 120, 100, and 75 $mAhg^{-1}$ at current densities of 0.2, 0.5, 1, 2, and 5 Ag^{-1} respectively (**Figure 3**a). Even at a very high current density of 10 Ag^{-1}, a capacity of ~50 $mAhg^{-1}$ is still maintained, demonstrating the excellent rate performance of the hollow carbon nanospheres based electrode. To the best of our knowledge, the presented results indicate the best rate performance ever measured for a sodium ion battery anode material.[8,11,12,15–19,21] The superior electrochemical performance of hollow carbon nanospheres is attributed to the specific characteristics of this unique hollow nanosphere structure and carbon shell ordering (Figure 3b). First of all, the well connected hollow carbon structure ensures an efficient and continuous electron transport. Secondly, a very defined and large electrode/ electrolyte contact area offers a large number of active sites for charge-transfer reaction. Thirdly, the large interlayer spacing facilitates sodium ion transport and storage between graphene layers, which is especially important for the larger sodium cation. Last but not least, the very thin shell thickness (< 12 nm) guarantees a very short sodium diffusion distance, which plays a vital role in the rate performance. To emphasize this point, a control experiment was performed using disordered hydrothermal carbons obtained from a saccharide precursor (i.e. D-Glucose) prepared without the addition of the morphology directing polystyrene latex template (SI, Figure S2–S4). At a low current density of 0.1 Ag^{-1}, the reversible capacity is approximately 137 $mAhg^{-1}$ much lower than that for the hollow nanosphere structure. With increasing current density, the capacity was observed to decrease rapidly for the non-hollow carbon material, under the same testing conditions. These results demonstrate that the favorable transport properties of this unique hollow nanosphere structure are essential for the superior electrochemical performance.

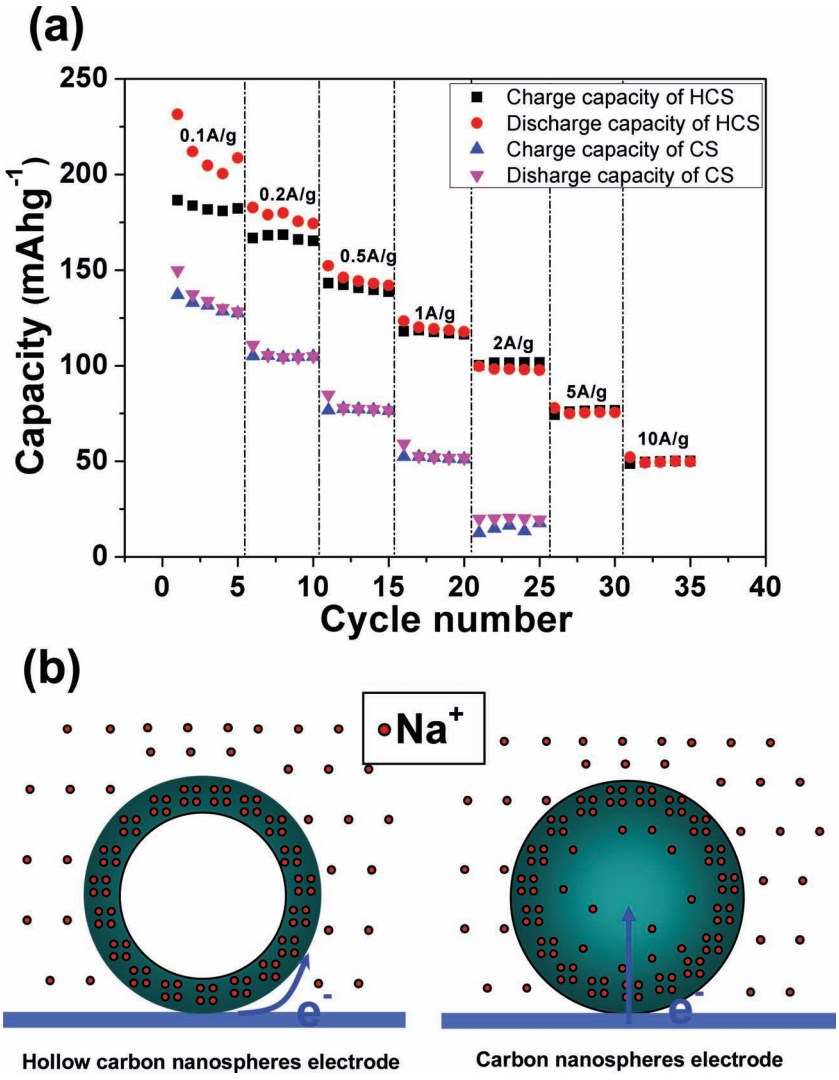

Figure 3. (a) Rate performance of hollow carbon nanospheres (HCS) and carbon spheres (CS) at variant rates. (b) Schemes of the electrochemical reaction process of hollow carbon nanospheres and carbon spheres.

In summary, we have demonstrated that hollow carbon nanospheres prepared by a facile, sustainable hydrothermal method possess excellent cycling stability and rate capability when employed as anode materials for the sodium-based battery. Further modification of material parameters such as morphology and size is an effective strategy by which to boost mass transport and storage, leading to a significant improvement of the electrochemical performance both for lithium and sodium. Our results represent the best level achieved so far and provide new perspectives concerning the possibility to construct low-cost sodium ion battery systems with Li-ion system competitive performance. As in the lithium system, these materials have to be improved in terms of irreversible capacity and volumetric energy density in order to make them good candidates for anodes.

Experimental Section

Synthesis of hollow carbon spheres: An aqueous dispersion of poly(styrene) latexes is mixed with D-Glucose acting as the carbon precursor. The solution was then sealed into the Teflon inlet in an

autoclave and hydrothermally treated at 180 °C for 20 h. After reaction, the carbonaceous product can be filtered off, followed by washing with excess H_2O and drying under vacuum. To remove the polymer template and to graphitise the carbonaceous shell, the composite material is then heated to 1000 °C.

Synthesis of hydrothermal carbons: D-Glucose dissolved in deionized water was used as starting solution. The solution was then sealed into the Teflon inlet in an autoclave and hydrothermally treated at 180 °C for 20 h. The obtained materials were filtered and washed several times with deionized water drying under vacuum. The dried precursors were calcined at 1000 °C under N_2 to obtain HTC carbons.

Characterization and Electrochemical measurements: Material morphology was visualized using a Zeiss Gemini DSM 982 scanning electron microscope (SEM).Transmission Electron Microscopy (TEM) was carried out with a Zeiss EM912 Omega operated at an acceleration voltage of 120 kV. The structure was characterized by X-ray diffraction (XRD) (Philips) using Cu Ka radiation. Nitrogen adsorption and desorption isotherms were measured at 77 K with a Quadrachrome Adsorption Instrument. Two-electrode Swagelok-type cells were used as testing batteries. The working electrode was made by spreading 85% hollow carbon spheres, 5% carbon black and 10% poly(vinylidene difluoride) (PVDF) onto a copper current collector and dried in a vacuum oven at 120 °C overnight. The cells were assembled in an argon-filled glove box. Sodium metal was utilized as counter electrode and glass fiber (GF/D) from Whatman was used as a separator. The electrolyte was 1 M $NaClO_4$ in propylene carbonate. Cyclic voltammetry measurements were performed on VoltaLab 80 electrochemical workstation at a scan rate of 0.1 mVs^{-1}. Electrochemical impedance measurements were also performed on VoltaLab 80 electrochemical workstation in the frequency range from 100 kHz to 0.01 Hz, and the voltage perturbation was controlled at 10 mV. Charge/discharge (0.001–3 V) tests were performed on an Arbin MSTAT battery test system under ambient temperature.

Supporting Information

Supporting Information is available from the Wiley Online Library or from the author. It includes the equivalent circuit used for fitting the experimental EIS data, SEM, and TEM images and charge/discharge curves of carbon spheres without the use of morphology directing templates.

Acknowledgements

We thank G. Götz for the XRD measurements. Dr. Noriko Yoshizawa, (AIST, Tsukuba, Japan) is thanked for the HR-TEM. We are indebted to the Max Planck Society and acknowledge support in the framework of the ENERCHEM project.

Received: November 16, 2011
Revised: January 30, 2012
Published online: May 21, 2012

[1] J. M. Tarascon, *Nat. Chem.* **2010**, *2*, 510.
[2] M. S. Whittingham, *Prog. Solid State Chem.* **1978**, *12*, 41.
[3] A. Nagelberg, W. L. Worrell, *J. Solid State Chem.* **1979**, *29*, 345.
[4] C. Delmas, J. Braconnier, C. Fouassier, P. Hagenmuller, *Solid State Ionics* **1981**, **3**, 165.
[5] J. M. Tarascon, G. W. Hull, *Solid State Ionics* **1986**, *22*, 85.
[6] S. Komaba, C. Takei, T. Nakayama, A. Ogata, N. Yabuuchi, *Electrochem. Commun.* **2009**, *12*, 355.
[7] S. Park, Gocheva, S. Okada, J.Yamaki, *J. Electrochem. Soc.* **2011**, *158*, A1067.
[8] S. Komaba, W. Murata, T. Ishikawa, N. Yabuuchi, T. Ozeki, T. Nakayama, A. Ogata, K. Gotoh, K. Fujiwara, *Adv. Funct. Mater.* **2011**, *21*, 3859.
[9] P. Ge, M. Fouletier, *Solid State Ionics* **1988**, *28*, 1172.
[10] D. A. Stevens, J. R. Dahn, *J. Electrochem. Soc.* **2001**, *148*, A803.
[11] P. Thomas, D. Billaud, *Electrochim. Acta* **2002**, *47*, 3303.
[12] P. Thomas, D. Billaud, *Electrochim. Acta* **2001**, *46*, 3359.
[13] V. L. Chevrier, G. Ceder, *J. Electrochem. Soc.* **2011**, *158*, A1011.
[14] M. M. Doeff, Y. Ma, S. J. Visco, L. C. de Jonghe, *J. Electrochem. Soc.* **1993**, *140*, 169.
[15] P. Thomas, J. Ghanbaja, D. Billaud, *Electrochim. Acta* **1999**, *45*, 423.
[16] D. A. Stevens, J. R. Dahn, *J. Electrochem. Soc.* **2000**, *147*, 1271.
[17] R. Alcantara, J. M. Jimenez-Mateos, P. Lavela, J. L. Tirado, *Electrochem. Commun.* **2001**, *3*, 639.
[18] R. Alcantara, P. Lavela, G. F. Ortiz, J. L. Tirado, *Electrochem. Solid-State Lett.* **2005**, *8*, A222.
[19] J. Maier, *Nat. Mater.* **2005**, *4*, 805.
[20] Y. S. Hu, P. Adelhelm, B. M. Smarsly, S. Hore, M. Antonietti, J. Maier, *Adv. Funct. Mater.* **2007**, *17*, 1873.
[21] S. Wenzel, T. Hara, J. Janek, P. Adelhelm, *Energy Environ. Sci.* **2011**, *4*, 3342.
[22] S. B. Yang, X. L. Feng, L. J. Zhi, Q. A. Cao, J. Maier, K. Müllen, *Adv. Mater.* **2010**, *22*, 838.
[23] K. X. Wang, Z. L. Li, Y. G. Wang, H. M. Liu, J. S. Chen, J. Holmes, H. S. Zhou, *J. Mater. Chem.* **2010**, *20*, 9748.
[24] S. Yoon, A. Manthiram, *J. Phys. Chem. C* **2011**, *115*, 9410.
[25] K. Tang, R. J. White, X. Mu, M. M. Titirici, P. van Aken, J. Maier, *ChemSusChem* **2012**, *5*, 400.
[26] R.J. White, K. Tauer, M. Antonietti, M. M. Titirici, *J. Am. Chem. Soc* **2010**, *132*, 17360.
[27] N. Baccile, G. Laurent, F. Babonneau, F. Fayon, M. M. Titirici, M. Antonietti, *J. Phys. Chem. C* **2009**, *113*, 9644.
[28] A.Vishnyakov, P. I. Ravikovitch, A. V. Neimark, *Langmuir* **1999**, *15*, 8736.
[29] Y. Matsumura, S. Wang, J. Mondori, *J. Electrochem. Soc* **1995**, *142*, 2914.
[30] M. Arakawa, J. I. Yamaki, *J. Electroanal. Chem.* **1987**, *219*, 273.
[31] J. Li, V. Mauricea, J. Mrowiecka, A. Seyeux, S. Zanna, L. Klein, S. Sun, P. Marcusa, *Electrochim. Acta* **2009**, *54*, 3700.
[32] Y. Marcus. *Pure Appl. Chem.* **1985**, *57*, 1129.
[33] J. R. Dahn, T. Zheng, Y. Liu, J. S. Xue, *Science* **1995**, *270*, 590.
[34] V. Subramanian, H. Zhu, B. Wei, *J. Phys. Chem. B.* **2006**, *110*, 7178.
[35] H. Yan, X. Huang, H. Li, L. Chen, *Solid State Ionics* **1998**, *11*, 113.